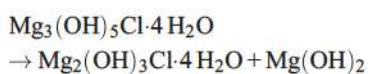# Chlorartinite, a volcanic exhalation product also found in industrial magnesia screed
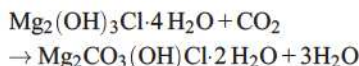
K. Sugimoto, R.E. Dinnebier and T. Schlecht

The pavement of high-quality industrial floors is mainly made from screed which is separated by a screening layer from the ferroconcrete of the base plate. Self leveling screed floors are easy to handle but require intensive and careful after-treatment. Generally, screed consists of aggregates, water, additives and binder. Depending on the required load, the largest differences between the different floor pavements are due to their binders. The most important binders are cement, anhydrite and calcium sulfate, mastic asphalt and magnesia. Typically, the binder makes up to about 15–25 wt% of the entire floor. Depending on the production and the setting process, the aging, and environmental influences, a variety of phases forms. With time, a typical floor not only consists of the original phases but also of degradation products. Manufacturers will be able to control the durability of the floor, if it is possible to clarify this process. Although wet chemical analysis provides some insight in the distribution of elements, the mineralogical composition is much more meaningful. In order to control the production or to evaluate structural damages in the construction business, a full quantitative phase analysis (QPA) using the Rietveld method is necessary, for which the knowledge of the crystal structures of the components is essential. The raw screed typically consists of quartz sand, technical magnesium oxide, technical magnesium chloride, inorganic pigments (usually iron oxides) and eventually kaolonite or other minerals to insure a proper workability of the mortar. After the binding and the consecutive drying process, a variety of magnesium hydroxide, magnesium chloride hydroxide and magnesium chloride hydroxide hydrate phases forms, of which at least 16 are reported in the ICDD database. For some of these compounds the crystal structure is missing, making a full QPA impossible.

The most important binder phases in industrial magnesia screed floors are $Mg(OH)_2$ (magnesium hydroxide), $Mg_3(OH)_5Cl\cdot4H_2O$ ('F5'-Phase), $Mg_2(OH)_3Cl\cdot4H_2O$ ('F3'-Phase), and $Mg_2(CO_3)OHCl\cdot3H_2O$ (Chlorartinite). The formation of the latter can be explained by the degradation of the F5 phase according to:

$$Mg_3(OH)_5Cl\cdot4H_2O$$
$$\rightarrow Mg_2(OH)_3Cl\cdot4H_2O + Mg(OH)_2$$

and consecutively

$$Mg_2(OH)_3Cl\cdot4H_2O + CO_2$$
$$\rightarrow Mg_2CO_3(OH)Cl\cdot2H_2O + 3H_2O$$

The amount of chlorartinite present in the binder varies from < 0.1 up to 30 wt%. Usually, very little chlorartinite is formed over long periods of time. On the other hand, chlorartinite was detected after a drying time in air of only two weeks in the laboratory, suggesting that its formation is a relatively fast process Excess water is believed to be responsible for the formation of appreciable amounts of chlorartinite, possibly making it an indicator for bricolage.

In 1998, chlorartinite was also found as a naturally occurring mineral and was first described as an opaque white crystalline volcanic exhalation product on volcanic glass at the third cone of the Northern Breakthrough of the Main Tolbachik fracture eruption (1975-1976), Kamchatka, Russia. The name of chlorartinite as the chloride analog of artinite, named after the Italian mineralogist of E. Artini (1866-1928), was approved by IMA 1998.

Due to the lack of single crystals suitable for single crystal analysis, we determined its crystal structure from high-resolution synchrotron powder diffraction data using the technique of Monte Carlo simulated annealing and Rietveld refinement. Also, we performed a full quantitative phase analysis (QPA) using the Rietveld method for a real magnesia floor.

The sample of chlorartinite was synthesized by adding a 10 wt% solution of $(NH_4)HCO_3$ into a hot concentrated solution of magnesium chloride. Chlorartinite then precipitates after short time. The probe of the magnesia floor for quantitative analysis was drilled out of a one year old magnesia screed in an industrial manufacturing building. Pycnometric determination of the density of chlorartinite at $T = 295 K$ using a He-Pycnometer lead to a density of $1.63(3) g/cm^3$.

High resolution X-ray powder diffraction experiments were performed at the SUNY X3B1 and X16C beamlines of the National Synchrotron Light Source at Brookhaven National Laboratory. A structural starting model for Rietveld refinement was subsequently found with the Monte Carlo simulated annealing program FOX in space group $R3c$. The initial composition of chlorartinite $[Mg_2(OH)ClCO_3]\cdot 3 H_2O$ which was used as input for FOX was taken from the ICDD database (PDF 7-278). The CO_3 moiety was restrained assuming an ideal triangular geometry with a C–O bond length of 1.23 Å and an O–C–O angle of 120.0°. Although the preferred coordination number of the magnesium atom is known to be six the actual distribution of the ligands between chlorine and oxygen atoms was not known *a priori*. Thus, no further geometrical constraints were introduced in the simulated annealing process. Hydrogen atoms were neglected. After about 20 million cycles (approximately 24 hours on a 2 GHz standard PC), a promising starting model in terms of crystal packing was found and subjected to Rietveld refinement using the GSAS program. Starting values for the lattice parameters, the background, and the peak profile were taken from the corresponding LeBail fit. In order to stabilize the Rietveld refinement, the CO_3 moiety was treated as an almost rigid triangular entity with an overall temperature factor and strong restraints on bond lengths and bond angles. All other non-hydrogen atoms of Mg, Cl and

O were freely refined using isotropic temperature factors. No hydrogen atoms were introduced in the Rietveld refinement. Although quick convergence was reached, the temperature factors of two oxygen atoms bonded to the magnesium atom turned slightly negative. A comparison with the crystal structure of artinite suggested the presence of hydrogen atoms in form of OH and OH_2 groups depending on the position of the oxygen atoms at the free vertex of a MgO_6 octahedron or at the corner of two edge sharing MgO_6 octahedra. Since the position of the hydrogen atoms could not be refined from powder diffraction data, the occupancy of the relevant oxygen atoms was increased to 1.125 for OH and 1.25 for H_2O, taking into account the additional electron density from the hydrogen atoms. This little trick immediately turned the temperature factors of these oxygen atoms into positive. Subsequent difference-Fourier cycling found disordered oxygen atoms in the honeycomb like channels, which can be attributed to water molecules. Thus, the formula of chlorartinite as determined from powder diffraction changed to $[Mg_2(CO_3)(H_2O)(OH)]Cl\cdot H_2O$. The final Rietveld refinement converged nicely with maximum residuals in the electron density map between $-0.827 e\text{Å}^{-3}$ and $0.666 e\text{Å}^{-3}$. No inversion center was found, confirming $R3c$ as the correct space group. The final Rietveld plot is given in Fig. 74.
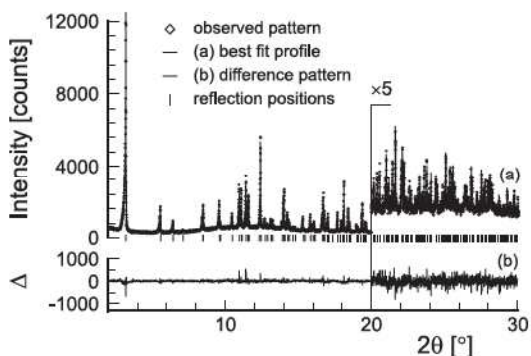

Figure 74: Rietveld plot of chlorartinite at $T = 295 K$. The high angle part starting at 20° (2θ) is enlarged by a factor of 5. The wavelength was $\lambda = 0.64889(2)$ Å.

Chlorartinite crystallizes in a complicated zeolite-like 3D-honeycomb framework structure with large 1D-channels running along c-direction. Chlorine atoms and disordered water molecules are located within the channels (Fig. 75). The two crystallographically distinct magnesium atoms are coordinated by distorted octahedra of the type $Mg(1)O_4(OH_2)(OH)$ and $Mg(2)O_5(OH)$. All Mg-polyhedra are connected to 5 neighboring Mg-polyhedra and to two triangular CO_3 groups sharing edges and corners. As building blocks of the channel walls, 15-membered puckered rings of Mg-polyhedra can be isolated where the triangular CO_3 moieties act as chelating ligangds. The perspective crystal packing of chlorartinite is shown in Fig. 75. The chlorine atoms and the disordered water molecules in the channels are clearly visible. The most embossed atom within the channel structure is O1, which the distance of O1···O1 is 6.454(15) Å. The disordered water molecules are located within the triangle which is formed by these oxygen atoms. The shortest contact distances between channel structure and captured atoms are: 3.000(10) Å for Cl1–O6[$-x+y, y, z-0.5$], 2.75(4) Å for O7–O1[$-y, x-y, z$], and 2.68(3) Å for O8–O1 [$-y, x-y, z$], allowing the formation of hydrogen bonds. Likewise, hydrogen bonds are also formed by the non-coordinated chlorine atom and the free water in the channels, with a contact distance of 3.064(19) Å between Cl1 and O8. Although chlorartinite $[Mg_2(CO_3)(H_2O)(OH)]Cl \cdot H_2O$ was named as the chloride analog of artinite, $[Mg_2(CO_3)(OH)_2] \cdot 3 H_2O$, its crystal structure is completely different from that of artinite, where the magnesium atoms are octahedrally surrounded by three hydroxyl groups, two water molecules and one oxygen atom which is disordered between water molecule and carbonate group. Instead of forming rings, the Mg-octahedra of Artinite are arranged in 1D double zig-zag chains running along b-axis and are stabilized by a complicated framework of hydrogen bonds. In contrast, the crystal structure of chlorartinite consists of a 3D-framework with large channels in a honeycomb fashion which captured free chlorine atoms and disordered water molecules. The chemical composition as found by the structure determination process differs slightly from previous reports in literature.
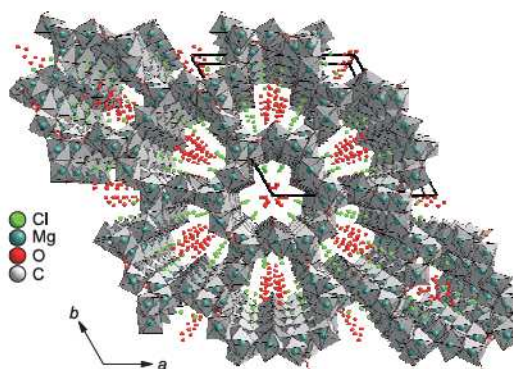

Figure 75: Perspective view of the crystal structure of chlorartinite in a central projection down to the crystallographic c-axis. Semi-transparent MgO_6 and CO_3 polyhedra are drawn.

A qualitative phase analysis of the synchrotron powder diffraction pattern of the industrial magnesia floor using the ICDD database revealed quartz (PDF 83-539), chlorartinite (PDF 7-278), calcite (PDF 83-577), microcline (PDF 76-1239) and clinotobermorite (PDF 88-1328). A QPA by the Rietveld method using the program GSAS revealed the following composition in weight%: 52.3(1)% for quartz, 28.9(2)% for chlorartinite, 9.9(1)% for microcline, 8.8(1)% for calcite and 0.13(3)% for clinotobermorite, respectively. The Rietveld plot of the QPA of the magnesia floor using a logarithmic intensity scale for better visibility of the minor phases is shown in Fig. 76. Quite unusually, the QPA of this particular sample revealed that literally all binder transformed into chlorartinite which might be caused by a bloomer during the blending or setting process of the screed.

Preliminary in situ synchrotron powder diffraction, DSC, TG and MAS on chlorartinite up to $T = 500°C$ revealed a variety of phase transitions within a small temperature range starting at $T = 125°C$ while decomposition into $Mg(OH)_2$ slowly starts at about $T = 190°C$.
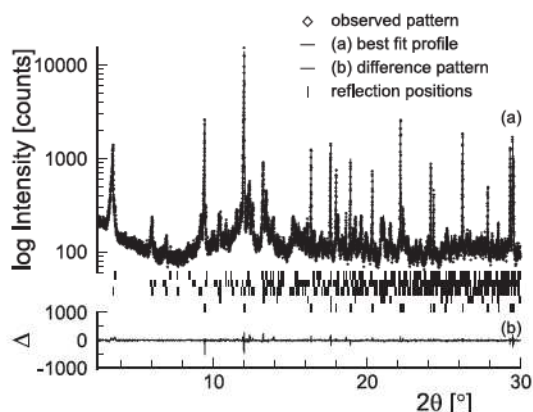
Figure 76: Rietveld plot (5 phases) of a magnesia screed at $T = 295$ K. The intensity is plotted on logarithmic scale. The wavelength was $\lambda = 0.70041(2)$ Å.

The different phases of chlorartinte are attributed to the step-wise loss of water molecules from the channel. It is interesting to note the water in the channels of chlorartinite is so loosely bound and that there is an immediate loss of crystal water if chlorartinite is exposed to a dry inert-gas stream at room temperature. This also explains the difference between the density of $1.63(3)$ g/cm^3 from a He-pycnometer and the X-ray density of 1.758 g/cm^3. Removing the water molecules would decrease the X-ray density to 1.597 g/cm^3 which is in excellent agreement to the pycnometrically determined value.

The ability of chlorartinite to quickly exchange crystal water along with a fast change in density of more than 15% makes it likely that industrial floors containing substantially amounts of chlorartinite are very sensitive to humidity conditions, leading to possible cracking damage. A quantitative analysis of chlorartinite can therefore be regarded as an indicator for the quality and the actual condition of these floors. We are currently in the process of collecting in situ powder diffraction data of chlorartinite in dependence on temperature- and humidity in order to fully understand the different phases of chlorartinite and their influence on the stability of magnesia floors.

Floating zone growth of lithium iron (II) phosphate single crystals

D.P. Chen, G. Götz and C.T. Lin

The need for compact, high-energy density, low cost, environmentally friendly and safe rechargeable batteries has led to the development of the lithium-polymer and lithium-ion battery concepts. During the past few years the search for cathode materials of rechargeable lithium batteries has focused mainly on lithium metal oxides. Among them, lithium iron phosphate, LiFePO$_4$, is one of the most promising candidates, since it provides an attractive voltage of 3.5 V, high theoretical capacity (170 mAhg^{-1}), low cost, ease of synthesis, and stability when used with common organic electrolyte systems. However, large, high-quality crystals have not been available up to now but are required for the study of the structural, physical and chemical properties, particularly for the electronic and magnetic anisotropies. Therefore, the growth of large and high-quality single crystals is of critical importance.

When sintering LiFePO$_4$, difficulties appear due to the oxidation and the high volatilization of Li at temperatures above 500°C. Moreover, the compound melts incongruently and readily decomposes during the sintering process, leading to a multiphase mixture of Fe$_2$O$_3$, Li$_3$PO$_4$ and Li$_3$Fe$_2$(PO$_4$)$_3$. Obviously, obtaining high-quality single crystals is rather difficult. In this contribution we present a floating zone method for preparing large and high-quality single crystals and demonstrate their structural behavior.